

# Oligomer-Nanoparticle Release from PLA Bioplastics Catalyzed by Gut Enzymes and Its Acute Inflammatory Effect

**Mengjing Wang**

School of Civil and Environmental Engineering, Nanyang Technological University

**Qianqian Li**

Key Laboratory of Environmental Nanotechnology and Health Effects, Research Center for Eco-Environmental Sciences, Chinese Academy of Sciences

**Youdong Xu**

State Key Laboratory of Proteomics, National Center for Protein Sciences – Beijing, Beijing Proteome Research Center, Beijing Institute of Lifeomics

**Junjie Yang**

School of Civil and Environmental Engineering, Nanyang Technological University

**Shae Linn Chua**

School of Materials Science and Engineering, Nanyang Technological University

**Linran Jia**

School of Civil and Environmental Engineering, Nanyang Technological University

**Jia Lv**

Department of Toxicology, School of Public Health; Key Laboratory of Environmental Toxicology of Anhui Higher Education Institutes, Anhui Medical University

**Huaiwen Chen**

Sunlipo Biotech Research Center for Nanomedicine

**Changjin Huang**

School of Mechanical and Aerospace Engineering, Nanyang Technological University

**Yichao Huang**

Department of Toxicology, School of Public Health; Key Laboratory of Environmental Toxicology of Anhui Higher Education Institutes, Anhui Medical University

**Jianmin Chen**

Fudan University <https://orcid.org/0000-0001-5859-3070>

**Mingliang Fang** (✉ [mlfang@ntu.edu.sg](mailto:mlfang@ntu.edu.sg))

Nanyang Technological University <https://orcid.org/0000-0002-2204-9783>

**Keywords:**

**Posted Date:** July 21st, 2022

**DOI:** <https://doi.org/10.21203/rs.3.rs-1844120/v1>

**License:**  This work is licensed under a Creative Commons Attribution 4.0 International License.

[Read Full License](#)

---

**Version of Record:** A version of this preprint was published at Nature Nanotechnology on March 2nd, 2023. See the published version at <https://doi.org/10.1038/s41565-023-01329-y>.

# Abstract

Although the risks of microplastics in environmental exposure and human health are being increasingly studied, little is known about the behavior of “eco-friendly” bioplastics in humans, especially their effects on our gastrointestinal tract. Here we demonstrate that enzymatic hydrolysis of bio-based polylactic acid (PLA) microplastics rapidly generates an excess of nanoplastic particles by competing for triglyceride-degrading lipase during gastrointestinal processes. These tiny nanoparticles are oligomers formed by hydrophobic-driven self-aggregation, and upon exposure the oligomers and their associated nanoparticles can bioaccumulate in *in vitro* and several *in vivo* organs, including the liver, intestine, and even in the brain. Severe intestinal damage and inflammation are also observed, the toxic effect of which is mostly pronounced from hydrolyzed oligomer products. Furthermore, the oligomers’ potential protein target screening using large scale pharmacophore model reveals that oligomers can interact with matrix metalloproteinase 12 protein (MMP12), which is further validated using protein binding assay. A close mechanistic study reveals high binding affinity of oligomers to the catalytic zinc ion finger domain, leading to MMP12 inactivation and mediating the adverse bowel inflammatory effect following PLA oligomer exposure. Since biodegradable plastics are highly proposed as one solution for the global plastic problem, understanding the gastrointestinal fate and toxicity of bioplastics, will provide ground-breaking data on bioplastics as a substantial risk to human health.

## Introduction

Microplastics (MPs) are ubiquitous in aquatic and terrestrial environment and the world’s most pressing environmental concerns <sup>1,2</sup>, due to their potential risk to the environment and human health <sup>3,4</sup>. MPs can not only be transferred in the environment and bioaccumulate through food chain, but also directly inhaled or ingested to human body. Studies estimating MP consumption via oral intake, the most common and major route <sup>5</sup>, ranges from 74,000–121,000 particles annually by humans around the world <sup>6</sup>. Accordingly, MPs have been detected in human stools <sup>7</sup>, serum <sup>8</sup>, and placenta <sup>9</sup>. Once MPs are ingested, serious physical and physiological threats may occur, including DNA damage, lipid peroxidation, gastrointestinal irritation, oxidative stress, and reproductive complications <sup>10</sup>. Studies in fish and mouse models have also shown that exposure to MPs can lead to a dysbiosis of the gut microbiota and a lipid metabolism disruption <sup>5,11,12</sup>. The mechanisms leading to these effects are often unknown, but many studies have probed the culprit being microplastics’ physical damage, reduced feeding amount, or the leaching of toxic chemicals <sup>3</sup>.

To alleviate plastic pollution, biodegradable plastics have been introduced as an environmentally friendly alternative to conventional plastics, as they can be readily degraded by microbial activity <sup>13</sup>. For example, polylactic acid (PLA), the most commonly used type of bioplastic, is used to manufacture food packaging materials, disposable plastic tableware, and delivery carriers for biomedical applications <sup>14</sup>. The production of PLA has increased steadily over the years, and is expected to exceed 300,000 tons by 2024 <sup>15</sup>. Degradable plastics are expected to be completely mineralized in the environment <sup>16</sup>, yet the

degradation of PLA requires specific conditions such as high temperature (58–80°C), high humidity (> 60%) and oxygen-rich environment<sup>17</sup>, hence the degradation of PLA has been proven to take longer than expected under natural environmental conditions<sup>18</sup>. Due to its relatively slow degradation rate, PLA can remain *in vivo* for typically 3–5 years<sup>19</sup>.

Studies in human and mouse model have shown PLA-based implantation triggered inflammatory reaction<sup>20</sup>. Some notable risks caused by PLA MPs have been demonstrated in zebrafish and earthworms<sup>21,22</sup>, albeit no specific underlying mechanism has been uncovered. Notwithstanding that the toxicological effects of the ingested biodegradable PLA warrant further study, our knowledge on how the bio-transformations of biodegradable microplastics (BMPs) in the gut may affect human health is still in its infancy. Our understanding of the extent to which these chemical structures of BMPs may be altered by this interaction under physiological conditions of low pH and enzymes, thereby increasing their bioreactivity and enhancing protein and cell surface interaction with BMPs is still lacking.

In this study, we explored the transformation and toxicity of PLA as a model BMP in the human gut. PLA MPs can be digested by the lipase enzyme in gastrointestinal tract, resulting in millions of nanoplastics. Moreover, biophysical and computational methods were employed to demonstrate that the hydrolysis product oligomers can organize themselves into nanoplastics. The biodistribution and histopathology of hydrolysis products were further studied *in vitro* and *in vivo* using cell and animal models. The potential protein targets of oligomers in causing inflammation were also investigated. In sum, in contrast to the conventional stable plastics, our work reveals that the unexpected degradation products including oligomers and nanoplastics from PLA bioplastics by gut enzymes have potential health risks that call for continued research and potential regulation.

## Results

### PLA MPs Degradation Through In vitro Digestive Model.

We first tested the degradation of PLA MPs under different digestive fluids. After artificial *in vitro* digestion in the stomach and intestinal fluids sequentially, the scanning electron microscopic (SEM) images revealed the PLA MPs' roughened surfaces (Fig. 1a), which may indicate biodegradation. SEM images also reveal the presence of hundreds of spherical particles with diameters of approximately 200 nm in suspension within the visual field (Fig. 1b). To determine which fluid was responsible for this breakdown, MPs were digested by stomach and intestinal fluids separately. On the surface of PLA MPs submerged in gastric fluid, no significant surface modification was noticed, whereas the surface of PLA MPs treated in intestinal fluid exhibited a comparable degree of degradation (Fig. S1). Hence, we hypothesized that lipase could hydrolyse PLA in the intestinal fluid likely due to the carboxylic ester linkages of PLA and the abundance of hydrolytic enzymes-lipase. The PLA-microplastics were biodegraded in PBS containing lipase at 37°C for three days, which is the amount of time required for food to pass through the digestive tract. In accordance with SEM analysis, the surface of the sample became more abrasive as the incubation time increased (Fig. 1c, Fig. S2). Further, the mass of PLA MPs

decreased rapidly to 85% of their initial mass after 6 hours (Fig. 1d). Buffer solution pH reduction was only observed in extremely high dose (100 mg/ml) group (Fig. S3). As a control, no change in mass and solution pH was observed for the conventional polystyrene (PS). In addition, there was no substantial change in the molecular and crystalline structures of residual PLA MPs before and after lipase treatment as confirmed by the gel permeation chromatography (GPC), Differential Scanning Calorimeter (DSC), X-ray diffraction (XRD), and Fourier-transform infrared (FTIR) spectroscopy (Figs. S4-S7).

To further evaluate the interaction between PLA and digestive lipases, we employed triglycerides as a positive control and examined the enzymatic competition for lipases. PLA demonstrates binding to digestive lipases and preventing triglyceride breakdown via competitive binding (Fig. 1e), yet no effect was observed in the supernatant of conventional PS plastics. In order to trace the uptake and translocation of plastic particles in complex biological media, PLA MPs were further fluorescently labelled by covalently reacting with fluorescein isothiocyanate (FITC) (Fig. 1f). The fluorescence intensity in the culture medium's supernatant is used as a proxy to evaluate the PLA degradation. The fluorescence signal enhanced significantly in the supernatant when PLA and lipases were used together compared to when treated alone, demonstrating PLA breakdown (Fig. 1g).

### **Nanoplastics released during digestion and its formation mechanism.**

The Nanoparticle Tracking Analysis (NTA) of the medium supernatant revealed that the number of PLA-nanoplastics peaked at  $8 \times 10^8$  particles/ml at 2 hours (Fig. 2a, Fig. S9). To determine the chemical nature of the released nanoparticles, atomic force microscopy-IR (AFM-IR) was conducted on the isolated nanoplastics generated from PLA MPs. The IR results confirmed that the formed nanoparticles were PLA, as illustrated by its characteristic band at  $1770 \text{ cm}^{-1}$  wave number corresponding to C = O stretching (Fig. 2b). The average size of PLA-nanoparticles was 200 nm after 2 h and 50 nm after one day of enzymatic hydrolysis (Fig. 2c), and plateaued over the next two consecutive days.

Interestingly, transmission electron microscopy (TEM) imaging revealed the formation of nanoplastics with several central cores, indicating that the particles may be self-aggregated as opposed to a single free-form particle (Fig. 2d). The size of the aggregated nanoplastic decreased significantly following dilution from dynamic light scattering (DLS) measurements (Fig. 2e). We also observed the size reduction of nanoparticles after adding Tween 20. To determine if PLA oligomers are capable of self-aggregation, we dissolved a synthesized oligomer with a molecular weight of 900 into PBS at a final concentration of 5 mg/ml, and a microscopic investigation revealed the presence of a significant number of particles (Fig. 2g). The GPC analysis of acetonitrile-dissolved nanoparticles in PBS supernatants showed presence of tiny peaks in the lower molecular weight range ( $\sim 900 \text{ Da}$ ) in the digested PLA (Fig. 2h), which are most likely leftover ester oligomers from the depolymerization. Further analysis of the precise oligomer units using high-resolution mass spectrometry indicated that 8-unit oligomer shows the greatest abundance (Fig. 2i), although accurate quantification cannot be performed due to a lack of standards.

In addition, we used molecular dynamic (MD) simulations to analyze the self-interactions of PLA oligomers, and revealed that affinities of this interaction were strongly dependent on the number of units, because the increasing number of units contributed to the hydrophobic interactions (Fig. 2j, Figs. S10-S11). This is consistent with the observed molecule weight in the HRMS and GPC analysis. The impact of the released PLA oligomers on the biological activity of lipase was also examined. MD simulations demonstrated that PLA oligomer occupied the active site of lipase by hydrogen bonding with the catalytic triad of Ser153, His264, and Asp177 (Fig. 2k, Fig. S12). Similarly, the affinities of PLA oligomers–lipase interactions were also highly dependent on the number of units, as increasing the number of units contributed to the formation of stronger hydrogen bonds (Fig. S13). The distance between the carboxyl carbon of PLA and the hydroxyl oxygen of Ser153 was closer than that of triglyceride, indicative of more accessible nucleophilic attack. Meanwhile, the binding affinity of triglyceride to the catalytic site is weaker than that of PLA oligomer due to the absence of a hydrogen bond.

In addition, in order to demonstrate how PLA oligomer binds to the catalytic site of lipase, we performed quantitative calculations for different catalytic conformations of PLA oligomer (Fig. S14). The transition state of PLA oligomer has a relative energy barrier of 0.11 eV, suggesting that once lipase's Ser153 nucleophilically approaches the carboxyl group, the subsequent catalytic steps may occur spontaneously. In sum, upon approaching to the catalytic site of lipase, PLA promotes stable binding at the catalytic site by hydrogen bonding, which not only prevents lipase from connecting to triglyceride but also reduces lipase activity.

### **The uptake of generated nanoparticles and oligomers *in vitro* and *in vivo*.**

We further predicted the bioavailability of PLA oligomers with different units using ADMETlab 2.0 server. The results revealed that shorter oligomers of PLA have advantageous bioavailability (Fig. S15). Next, to study whether the released nanoplastic or the oligomers can be taken up by liver cells *in vitro*, we treated the human liver cancer cell line HepG2 cells with fluorescence PLA-nanoplastics and fluorescence oligomer. Both images displayed high signal intensity and predominant intracellular localization, with PLA oligomers show higher signal (Fig. 3a). Those results suggested that both nanoparticles and oligomers can enter the cell *in vitro*.

To further understand the *in vivo* relevance of exposure to PLA-MPs, we administered mice with fluorescent PLA-MPs and fluorescent oligomer for one week and traced the tissue biodistributions of fluorescence products and the fate of PLA-MPs and oligomer in intestine content. Based on the current data that humans are estimated to ingest tens of thousands to millions of MP particles annually, or on the order of several milligrams daily <sup>6</sup>, we selected 1.0 mg/day PLA MPs and oligomers as the dose for mouse experiments. The fluorescence result showed that PLA was widely distributed in various tissues throughout the mouse body (Fig. 3b). Further, the ingested PLA MPs are fragmented into small fragments in the intestine of mice at submicron size (Fig. 3c), confirming the fragmentation and depolymerization process *in vivo*, though our fluorescence microscope could not resolve the particles in the nano scale. The signals for PLA-nanoparticles and oligomers mainly concentrated in the liver and intestinal/colon region

(Fig. 3d). Moreover, further *ex vivo* imaging analysis confirmed this observation (Fig. 3e). We also observed moderate signal abundance in the brain samples of both groups. Early experimental and predication data both suggested the penetration of the blood brain barrier of PLA oligomer<sup>23,24</sup>. MP sizes were clearly visible as distinct fluorescent spots in the liver, gut, and brain of exposed mice. In comparison, stronger signal in liver and intestine were observed in mice treated with oligomer compared with PLA MPs mice.

### **PLA oligomers induced inflammation in the liver and intestine.**

In order to understand the effect of PLA following acute oral exposure, the major accumulated tissues were then selected for toxicological examination. Representative histological sections of livers, small intestine and colon from mice were examined (Fig. 3f). Histopathological analysis revealed that mice treated with PLA-MPs produced inflammation and infiltrate in the livers, small intestine, and colon. Similarly, PAS staining of colon detected abolished goblet cell hyperplasia and mucus production in comparison with controls. Likewise, oligomer also caused these adverse effects, albeit with a higher efficacy. Biochemical analyses of proinflammatory cytokines, TNF- $\alpha$ , in the tissues of liver, small intestine, and colon all showed significant elevation and hence is consistent with the histological data (Fig. 3g).

### **Possible protein targets of oligomers in inducing inflammation.**

To figure out the potential mechanism for the inflammation, we first tested whether the bowel micro-environment pH was modulated as PLA digestion may release acidic group after hydrolysis. The result showed minimal potency changes in the buffer solution at the given doses (Fig. S3), suggesting that acidity is unlikely to explain the toxicity. We further hypothesized that oligomers regulate inflammation by directly interacting with some targeted inflammation regulating proteins. Albeit no available data in the literature on PLA oligomer-protein interaction, the protein binding affinity of octamer with 16,646 proteins using pharmacophore models (Fig. 4a, Table S2) were screened by consolidating GPC results and mass spectrometry data. The result showed that the PLA 8 units-Matrix Metalloproteinase 12 (MMP12) displayed the highest fitness score value of 1.974. Computational analysis further showed that the affinity strength to MMP12 catalytic site corresponding to oligomer unit length topped after 10 units (Fig. 4b, Figs. S16 and S17). We further discovered that as the PLA units increased, the carboxyl oxygen of PLA could interact with zinc ions via electrostatic attraction. Such electrostatic force starts to attenuate significantly as the oligomer unit number reaches 11. Thus, it is hypothesized that there are no favourable hydrophobic and hydrogen-bonding interactions between PLA oligomers and MMP12, and that their attraction is mostly due to the electrostatic contact between carboxyl oxygen and zinc ions.

To further validate this interaction experimentally, isothermal titration calorimetry (ITC) was conducted and the result showed that the calculated binding affinity  $K_d$  of the MMP12-pure PLA oligomer (Fig. 4c) and hydrolysis products (Fig. 4d) interaction was 13.3  $\mu$ M and 67.8  $\mu$ M, respectively. MMP12, as an enzyme to degrade extracellular matrix components, has a crucial role in regulating the response of inflammation<sup>25</sup>. For example, MMP12 dampens inflammation via terminating complement activation

and increases phagocytosis<sup>26</sup>. To study the immunotoxicity of oligomer, we measured the MMP-12 bioactivity, C3a, C5a, and TNF- $\alpha$  production by raw264.7 macrophages treated with a series of doses of oligomer. Cell viability were not affected by PLA-MPs, pure PLA oligomer, PLA hydrolysis products oligomer, or PLA-nanoplastics under tested doses (Fig. S18), yet MMP12 bioactivity was attenuated when treated with PLA oligomer of soluble hydrolysis products, accompanied by elevation in C3a, C5a, and TNF- $\alpha$  levels (Figs. 5b, 5d). Exposure to PLA-MPs and PLA-nanoplastics demonstrated a tendency of MMP12 bioactivity reduction, and C3a, C5a, and TNF- $\alpha$  escalation (Figs. 5a, 5c). Our *in vivo* phenotypic data confirmed the findings that mice treated with PLA MPs and PLA oligomers demonstrated similar MMP12 bioactivity decrease, but increase in C3a and C5a levels in the liver, small intestine, and colon (Figs. 5e-5g). Notably, oligomers resulted in more significant inflammatory effect, which further confirms the immune regulation effect of oligomers.

## Discussion

Biodegradable plastics has been proposed as one major solution for the conventional “persistent” plastic issue; however, whether these replacements pose a substantial risk to human health is far from being understood. Humans ingest a substantial amount of bioplastics, and once ingested our gastrointestinal tract can directly alter their initial chemical structures, thus modifying their lifetimes, bioavailability, and biological effects. Although bioplastics has been known to be degraded in the natural environment, our knowledge on how gut transformations of bioplastic and its associated human health is still at early stage. Here we show that the mass of PLA MPs rapidly reduces by 6% of the initial thickness after 2 h of biodegradation with gut enzymes. PLA nanoplastics are produced rapidly during lipase degradation under digestive conditions from PLA MPs. The fact that PLA can be the substrates for triglycerides lipases has significant human relevance and health concern. The release of nano-sized bioplastic particles is faster than expected, with peak PLA nanoplastics formation after only two hours’ enzymatic hydrolysis, as opposed to the longer time needed for other bioplastics<sup>27,28</sup> and conventional plastics<sup>29,30</sup>. Our observations suggest that nanoplastics released from a biodegradable polymer during digestion is in more complex ways than has been previously appreciated.

In addition, we propose a novel potential formation mechanism of nanoplastic during the digestion, which may be manifested with greater toxicity than the micro-sized plastic particles. During the enzymatic hydrolysis process, hydrolytic products such as oligomers are also released and self-assembled into nanoplastics. UV and high-temperature water fragmentation are significant daily processes that contribute to the *in situ* formation of nanoparticles, but mostly in the few hundred nm range and with smaller quantity<sup>4,31,32,33</sup>. These results provide a new finding that human gut might contribute to the much smaller nanoplastic (~ 50 nm) during passing through digestive system. Limited *in vitro* and *in vivo* data imply that absorption patterns and uptake efficiency often increase with particle size reduction<sup>34</sup>. The particles (< 0.1  $\mu$ m) may be capable of accessing all organs, crossing cell membranes<sup>34</sup>, the placenta<sup>35</sup>, and also the brain<sup>35</sup>. This incredibly small nanoplastics allows them to

permeate the gastrointestinal tract more easily, allowing them to enter the circulatory system, reaching other tissues, and further induce intestinal health risks, such as inflammation.

Another intriguing result in this study is the mechanism underlying PLA oligomer's deleterious effect and its mode of action. Here, we have demonstrated direct inhibitory effects of PLA oligomers on lipase activity. The PLA can effectively compete for binding with lipases against the designated substrate triglycerides. Research on conventional microplastics have shown that lipid digestion was greatly reduced by using five MPs, including PS, PET, polyethylene, polyvinyl chloride, and poly(lactic-co-glycolic acid)<sup>36</sup>. PS MPs are suggested to generate large quantity of lipid-MPs hetero-aggregates, and lipase was persistently adsorbed to the PS surface hence decrease in activity. However, the quantity of PLA is generally much smaller than the dietary fat and the human implication on the digestion and absorption of lipids still needs more validation at population scale.

We further examined these generated nanoplastics and fragmented oligomers for toxicological effects. Several studies have demonstrated the ability of nanoplastics to distribute into the blood, placenta, brain, and feces<sup>5, 8, 9, 37</sup>, whereby the exposure particle size was sufficiently small to achieve bio-translocation. Our work further shows that oligomers seem to be more bioavailable in cells. Higher biodistribution of PLA oligomers was observed in brain compared with their original BMPs. This might be attributed to the size advantage of PLA nanoparticles or oligomers capable of passing the BBB and transcytosis by microvascular endothelial cells<sup>23</sup>. These computational results also indicated that shorter polymer chain lengths are more easily accumulated due to small molecular size. Nonetheless, data on the formation and toxicity of oligomers is quite lacking for the polymers. Despite the properties of pristine polymers, all plastics especially the biodegradable types, even those with chemical stabilizers, will eventually degrade in the environment<sup>38</sup>. Some previous studies have revealed that the oligomers in the polymer are likely the main contributors for the polymer toxicity<sup>39, 40</sup>. Our study hereby reinforces a previously underestimated dynamic in the plastic pollution threat, with the implication that biological fragmentation of microplastics may be widespread within ecosystems and human. As such, the harmful effects of plastic pollution must take into consideration not only the physical effects of microplastics and nanoplastics *per se*, but also the potential cellular effects of plastics oligomer and the bio-magnification impacts on the ecosystem thereon.

Very few toxicological studies investigated the health effects of PLA microplastics, let alone the under-reported metabolites PLA-oligomers, hence this study provides a new molecular understanding of the PLA degraded oligomers in the etiology of bowel inflammation. We have observed severe inflammation in the intestine and colon in the mice exposed to PLA MPs. Of note, the observed inflammation is likely induced by the oligomers, due to hydrolysis and re-formation, rather than the direct particle fragments from PLA. It was held that the biodegradation of PLA can lead to massive immune cell infusion and inflammation<sup>41</sup>, due to the acidic properties of their degradation products. However, the pH of the digestive fluid remains unchanged in our experiment, suggesting a minimal role of pH in the inflammation in the intestinal, consistent with other studies on the neutral pH of the intestinal environment of orally delivered

poly(lactic-co-glycolic) acid nanoparticles (12 mg/kg/animal/day orally for 21 day) <sup>42</sup>. Using octamers as a major oligomer in the PLA hydrolysis, we used *in silico* ligand-protein interaction models to screen the possible targets among most well-known pharmaceutical target proteins. Together with experimental validation, we have confirmed that inactivation by PLA oligomers of the key immune modulators MMP12 may provide a novel explanation of PLA's role in immune modulation. MMP12 is identified as a key mediator that sets the stage for resolution of inflammation due to its major role in controlling the tissue tightness and permeability. MMP12 inactivates complement C3 to reduce complement activation and inactivates the chemoattractant anaphylatoxins C3a and C5a <sup>26</sup>. Such direct PLA oligomers-MMP12 interplay offers new insight for the inflammation induced by PLA (Fig. 6). Further investigations are still warranted to examine the role of MMP12 inhibition by other oligomers and its human health relevance.

To the best of our knowledge, assessments of human exposure to microplastics have not included short chain microplastic polymers, nor the potentially toxic oligomers. Consumer plastic products, including polypropylene feeding bottles <sup>4</sup>, silicone-rubber baby teats <sup>33</sup>, nylon bags and hot beverage cups <sup>43</sup>, and plastic teabags <sup>44</sup> may have released trillions of nanoplastics, but not included further breakdown of nanoplastics, and even the potentially more toxic oligomers. This may have underestimated the total exposure volume to microplastics. Our results, taken together, add to the understanding on how degrading products of biodegradable plastics can act as toxic pollutants towards organisms.

## Methods

### Lipase hydrolyses PLA MPs

The lipase (20 mg/ml) in PBS were prepared by filtering insoluble fraction using 0.45 µm Acrodisc syringe filter. Subsequently, filtered lipase were exposed to the indicated doses of PLA MPs at 37°C. Sodium azide was used as an antibacterial agent. MPs spiked in inactivated lipase were used as the control. Lipase was deactivated by heating in water bath at 90°C for 10 min. The degraded PLA MPs were carefully filtered from the solution, and washed with 1% SDS, distilled water, and ethanol, then dried in a desiccator containing silica gel. At each indicated time, the changes in appearance, mass, GPC, DSC, XRD, FTIR of degraded PLA MPs, and the change in pH of buffer solution were evaluated. Lipase specific activity was assayed by using lipase kit (Nanjing Jiancheng Bioengineering Institute, No. A054-1).

### Physical and chemical characterizations of PLA hydrolysis products

The profiling of PLA hydrolysis products was conducted using a high performance liquid chromatography (HPLC) system (Agilent Technologies, Singapore) coupled to a 6550 Q-TOF (Agilent Technologies, Singapore), in accordance with one previous study <sup>45</sup>. Briefly, the samples were separated using one reverse phase chromatography and analyzed using electro-spray ionization positive mode

together with data-dependent MS/MS fragmentation acquisition. The predicted oligomers ranging from one to ten units were extracted from the high-resolution data and further confirmed with tandem mass spectrometry (MS/MS) fragmentation pattern. Prior to sample analysis, the solution was filtered first with a 1.0 µm PTFE filter to remove the plastic particles and then with a Vivaspın® 20, 3 kDa MWCO Polyethersulfone membrane (Merck, Singapore) to remove the enzymes in the solution by membrane ultrafiltration in a centrifuge. PLA-nanoplastics (free in suspension) were obtained by filtering using 1.0 µm syringe filter. The nanoplastic was characterised by SEM (FESEM, JEOL JSM-7600F) and transmission electron microscope (TEM, FEI Titan G<sup>2</sup> 60–300). Dynamic light scattering (DLS) measurements were done with a Zetasizer Nano ZS (Malvern Instruments, Malvern, UK). Nanoparticle tracking analyses (NTA) measurements were performed using a NanoSight NS300 (Malvern Instruments, Malvern, UK) equipped with a 488 nm laser. The Atomic Force Microscopy-Infrared Spectroscopy (AFM-IR) data were collected with a NanoIR2-fs (Bruker Corporation) instrument to study the type of nanoplastics.

## **In vivo PLA MPs and PLA oligomers challenge.**

The animal studies were conducted under protocols approved by the Animal Ethics Committee of the Research Center for Eco-Environmental Sciences, Chinese Academy of Sciences (AEWC-RCEES-2021001). Five-week-old male mice (n = 5 mice, each treatment) were housed in stainless-steel cages and acclimated for 1 week at 25 ± 4°C, 50 ± 5% relative humidity, and a 12/12 h light/dark cycle. Food and water were provided *ad libitum*. 10 mg FITC-labelled PLA MPs and FITC-labelled PLA oligomers were dispersed in 5 mL PBS, then 0.5 mL of the mixed solution was given once daily (1.0 mg/day) by oral gavage for 7 days. PBS only was used as a negative control. Mice was sacrificed one day after exposed to MPs. Organs including brain, liver, spleen, kidneys, small intestine, and colon were collected for biodistribution and histopathology studies.

## **In vitro PLA MP and PLA oligomer challenge.**

RAW264.7, a mouse macrophage cell line, was cultured in high-glucose Dulbecco's modified Eagle's medium (DMEM) containing 10% fetal bovine serum (FBS), 100 U/ml penicillin, and 100 µg/ml streptomycin at 37°C in a humidified incubator containing 5% CO<sub>2</sub>. RAW 264.7 macrophages were exposed to test PLA MPs, PLA nanoplastics, PLA hydrolysis products oligomers, and PLA oligomers or dimethyl sulfoxide (DMSO; 0.1% final concentration) for 24 h. Cell viability was measured using the MTT assay. The bioactivity of MMP12, and the concentrations of C3a, C5A, and TNF-α in culture supernatants were determined using ELISA kits.

## **Statistical Analysis.**

Data presented as the mean  $\pm$  standard error of the mean (and S.E.M) represent at least three independent experiments. For experiments using mice, we calculated the difference between groups using *Student's t* test or a one-factor analysis of variance (*ANOVA*) with Duncan's post-hoc test. The significance level was set at  $*p < 0.05$ , and  $**p < 0.01$ .

## Declarations

### Acknowledgments

This work was primarily supported by Singapore Ministry of Education Academic Research Fund (M4011732.030), Fudan Start-up grant (JIH1829010Y), and the National Natural Science Foundation of China (81900071, 82173484, 92043301).

### Author Contributions

M.J.W., Y.C.H., J.M.C., M.L.F. designed the study; Q.Q.L., Y.D.X., J.J.Y., S.L.C., L.R.J., H.W.C., J.L., C.J.H. performed the experiments; M.J.W., Y.C.H., J.M.C., and M.L.F. analysed the data and wrote the paper.

**Competing interests.** The authors declare no competing interests.

### Supplementary Information.

This file contains the Supplementary Materials and Methods, Supplementary Figures S1-S18, and Supplementary Tables S1-S2.

## References

1. Hurley R, Woodward J, Rothwell JJ. Microplastic contamination of river beds significantly reduced by catchment-wide flooding. *Nat Geosci* **11**, 251–257 (2018).
2. Galloway TS, Cole M, Lewis C. Interactions of microplastic debris throughout the marine ecosystem. *Nat Ecol Evol* **1**, 0116 (2017).
3. Koelmans AA, Redondo-Hasselerharm PE, Nor NHM, de Ruijter VN, Mintenig SM, Kooi M. Risk assessment of microplastic particles. *Nat Rev Mater* **7**, 138–152 (2022).
4. Li D, *et al.* Microplastic release from the degradation of polypropylene feeding bottles during infant formula preparation. *Nat Food* **1**, 746–754 (2020).
5. Yan Z, Liu Y, Zhang T, Zhang F, Ren H, Zhang Y. Analysis of Microplastics in Human Feces Reveals a Correlation between Fecal Microplastics and Inflammatory Bowel Disease Status. *Environ Sci Technol* **56**, 414–421 (2021).
6. Kannan K, Vimalkumar K. A review of human exposure to microplastics and insights into microplastics as obesogens. *Front Endocrinol* **12**, 724989 (2021).

7. Schwabl P, *et al.* Detection of various microplastics in human stool: a prospective case series. *Ann Intern Med* **171**, 453–457 (2019).
8. Leslie HA, van Velzen MJM, Brandsma SH, Vethaak AD, Garcia-Vallejo JJ, Lamoree MH. Discovery and quantification of plastic particle pollution in human blood. *Environ Int* **163**, 107199 (2022).
9. Ragusa A, *et al.* Plasticenta: First evidence of microplastics in human placenta. *Environ Int* **146**, 106274 (2021).
10. Prokić MD, Radovanović TB, Gavrić JP, Faggio C. Ecotoxicological effects of microplastics: Examination of biomarkers, current state and future perspectives. *Trends Analyt Chem* **111**, 37–46 (2019).
11. Mattsson K, Johnson EV, Malmendal A, Linse S, Hansson L-A, Cedervall T. Brain damage and behavioural disorders in fish induced by plastic nanoparticles delivered through the food chain. *Sci Rep* **7**, 1–7 (2017).
12. Jin Y, Lu L, Tu W, Luo T, Fu Z. Impacts of polystyrene microplastic on the gut barrier, microbiota and metabolism of mice. *Sci Total Environ* **649**, 308–317 (2019).
13. Yu Y, Griffin-LaHue DE, Miles CA, Hayes DG, Flury M. Are micro-and nanoplastics from soil-biodegradable plastic mulches an environmental concern? *J Hazard Mater Adv* **4**, 100024 (2021).
14. Aznar M, Ubeda S, Dreolin N, Nerin C. Determination of non-volatile components of a biodegradable food packaging material based on polyester and polylactic acid (PLA) and its migration to food simulants. *J Chromatogr A* **1583**, 1–8 (2019).
15. Ncube LK, Ude AU, Ogunmuyiwa EN, Zulkifli R, Beas IN. Environmental Impact of Food Packaging Materials: A Review of Contemporary Development from Conventional Plastics to Polylactic Acid Based Materials. *Materials (Basel)* **13**, 4994 (2020).
16. Karamanlioglu M, Preziosi R, Robson GD. Abiotic and biotic environmental degradation of the bioplastic polymer poly (lactic acid): A review. *Polym Degrad Stab* **137**, 122–130 (2017).
17. Chrysafi I, Ainali NM, Bikiaris DN. Thermal Degradation Mechanism and Decomposition Kinetic Studies of Poly(Lactic Acid) and Its Copolymers with Poly(Hexylene Succinate). *Polymers (Basel)* **13**, 1365 (2021).
18. Xu J, Zhang K, Wang L, Yao Y, Sun H. Strong but reversible sorption on polar microplastics enhanced earthworm bioaccumulation of associated organic compounds. *J Hazard Mater* **423**, 127079 (2022).
19. DeStefano V, Khan S, Tabada A. Applications of PLA in modern medicine. *ER* **1**, 76–87 (2020).
20. Ramot Y, Haim-Zada M, Domb AJ, Nyska A. Biocompatibility and safety of PLA and its copolymers. *Adv Drug Deliv Rev* **107**, 153–162 (2016).
21. Zhang X, *et al.* Photolytic degradation elevated the toxicity of polylactic acid microplastics to developing zebrafish by triggering mitochondrial dysfunction and apoptosis. *J Hazard Mater* **413**, 125321 (2021).
22. Duan Z, *et al.* Diet preference of zebrafish (*Danio rerio*) for bio-based polylactic acid microplastics and induced intestinal damage and microbiota dysbiosis. *J Hazard Mater* **429**, 128332 (2022).

23. Wang HF, Hu Y, Sun WQ, Xie CS. Polylactic acid nanoparticles across the brain-blood barrier observed with analytical electron microscopy. *Chin J Biotechnol* **20**, 790–794 (2004).
24. Dascalu D, Roman DL, Filip M, Ciorsac A, Ostafe V, Isvoran A. Solubility and ADMET profiles of short oligomers of lactic acid. *ADMET DMPK* **8**, 425–436 (2020).
25. Collison J. MMP12 makes the cut. *Nat Rev Rheumatol* **14**, 501 (2018).
26. Bellac CL, *et al.* Macrophage matrix metalloproteinase-12 dampens inflammation and neutrophil influx in arthritis. *Cell Rep* **9**, 618–632 (2014).
27. Wei XF, *et al.* Millions of microplastics released from a biodegradable polymer during biodegradation/enzymatic hydrolysis. *Water Res* **211**, 118068 (2022).
28. González-Pleiter M, *et al.* Secondary nanoplastics released from a biodegradable microplastic severely impact freshwater environments. *Environ Sci Nano* **6**, 1382–1392 (2019).
29. Lambert S, Wagner M. Characterisation of nanoplastics during the degradation of polystyrene. *Chemosphere* **145**, 265–268 (2016).
30. Lambert S, Wagner M. Formation of microscopic particles during the degradation of different polymers. *Chemosphere* **161**, 510–517 (2016).
31. Mattsson K, Björkroth F, Karlsson T, Hassellöv M. Nanofragmentation of expanded polystyrene under simulated environmental weathering (thermooxidative degradation and hydrodynamic turbulence). *Front Mar Sci* **7**, 1252 (2021).
32. Sorasan C, *et al.* Generation of nanoplastics during the photoageing of low-density polyethylene. *Environ Pollut* **289**, 117919 (2021).
33. Su Y, *et al.* Steam disinfection releases micro (nano) plastics from silicone-rubber baby teats as examined by optical photothermal infrared microspectroscopy. *Nat Nanotechnol* **17**, 76–85 (2022).
34. Wright SL, Kelly FJ. Plastic and Human Health: A Micro Issue? *Environ Sci Technol* **51**, 6634–6647 (2017).
35. Gruber MM, *et al.* Plasma proteins facilitates placental transfer of polystyrene particles. *J Nanobiotechnology* **18**, 128 (2020).
36. Tan H, Yue T, Xu Y, Zhao J, Xing B. Microplastics Reduce Lipid Digestion in Simulated Human Gastrointestinal System. *Environ Sci Technol* **54**, 12285–12294 (2020).
37. Browne MA, Dissanayake A, Galloway TS, Lowe DM, Thompson RC. Ingested microscopic plastic translocates to the circulatory system of the mussel, *Mytilus edulis* (L). *Environ Sci Technol* **42**, 5026–5031 (2008).
38. Dawson AL, *et al.* Turning microplastics into nanoplastics through digestive fragmentation by Antarctic krill. *Nat Commun* **9**, 1001 (2018).
39. Ubeda S, Aznar M, Alfaro P, Nerin C. Migration of oligomers from a food contact biopolymer based on polylactic acid (PLA) and polyester. *Anal Bioanal Chem* **411**, 3521–3532 (2019).
40. Fan P, Yu H, Xi B, Tan W. A review on the occurrence and influence of biodegradable microplastics in soil ecosystems: Are biodegradable plastics substitute or threat? *Environ Int* **163**, 107244 (2022).

41. Manavitehrani I, Fathi A, Wang Y, Maitz PK, Dehghani F. Reinforced Poly(Propylene Carbonate) Composite with Enhanced and Tunable Characteristics, an Alternative for Poly(lactic Acid). *ACS Appl Mater Interfaces* **7**, 22421–22430 (2015).
42. Navarro SM, *et al.* Biodistribution and toxicity of orally administered poly (lactic-co-glycolic) acid nanoparticles to F344 rats for 21 days. *Nanomedicine (Lond)* **11**, 1653–1669 (2016).
43. Zangmeister CD, Radney JG, Benkstein KD, Kalanyan B. Common Single-Use Consumer Plastic Products Release Trillions of Sub-100 nm Nanoparticles per Liter into Water during Normal Use. *Environ Sci Technol* **56**, 5448–5455 (2022).
44. Hernandez LM, Xu EG, Larsson HC, Tahara R, Maisuria VB, Tufenkji N. Plastic teabags release billions of microparticles and nanoparticles into tea. *Environ Sci Technol* **53**, 12300–12310 (2019).
45. Hajighasemi M, *et al.* Biochemical and structural insights into enzymatic depolymerization of polylactic acid and other polyesters by microbial carboxylesterases. *Biomacromolecules* **17**, 2027–2039 (2016).

## Figures

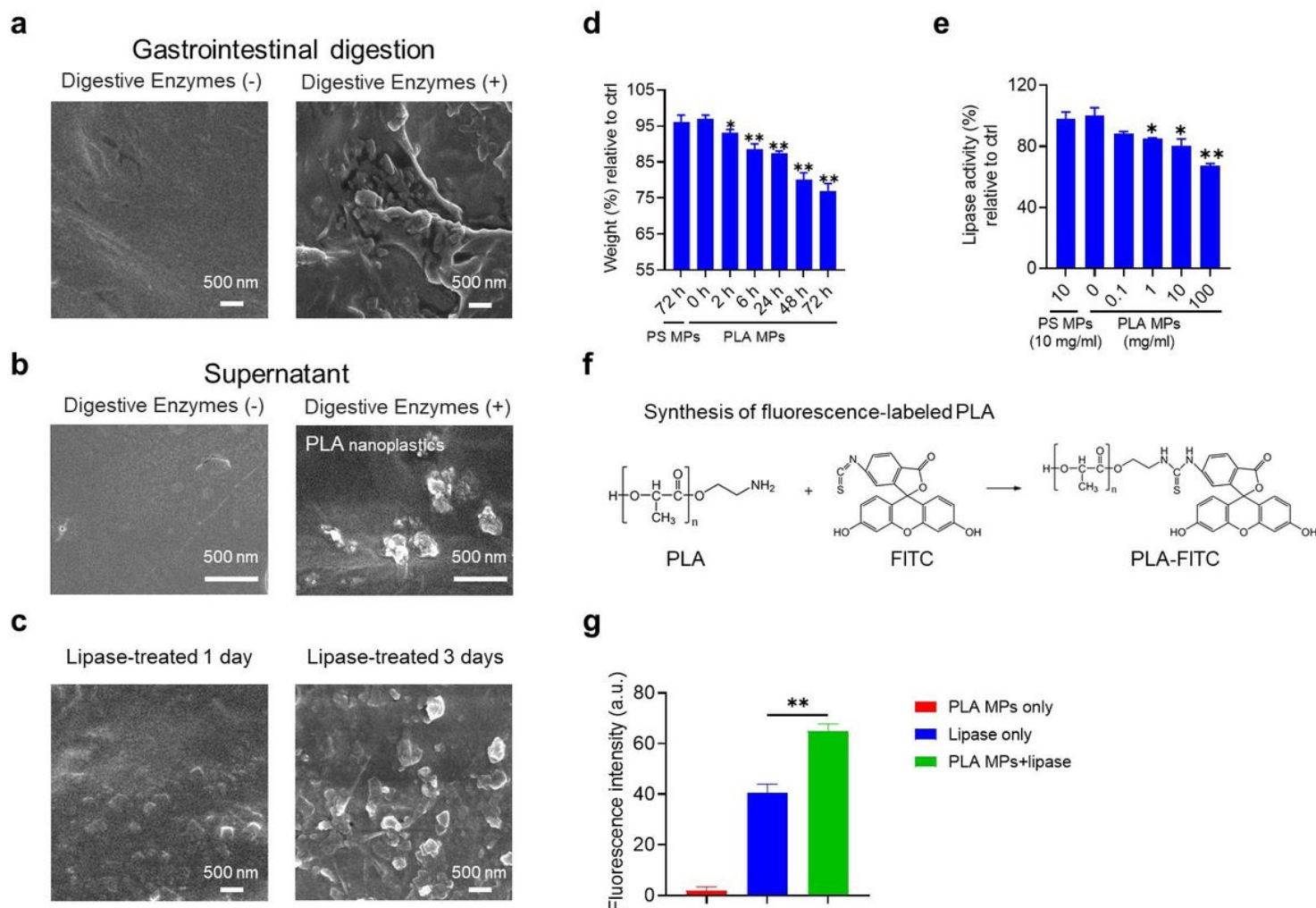
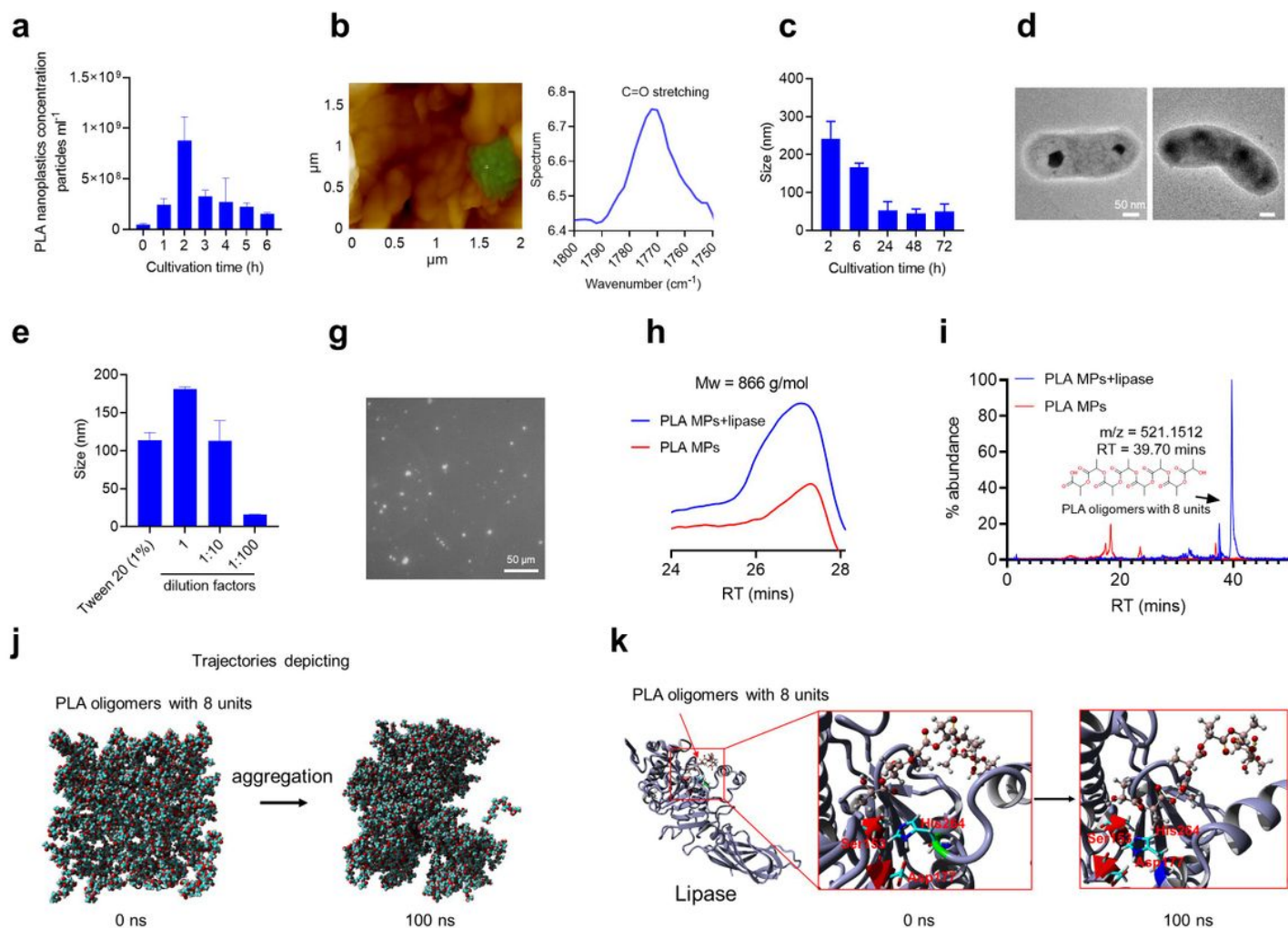


Figure 1

**Human gastrointestinal tract digests PLA MPs.** **a** Scanning electron microscope (SEM) images of PLA MPs after 3 days of digestion without (-) and with (+) enzyme. **b** SEM images of PLA-nanoplastics (free in supernatant) formed during the digestion. **c** SEM images of PLA MPs after 1 day and 3 days of biodegradation by lipase. **d** Changes in the mass of the PLA MPs and PS MPs during the biodegradation by lipase. **e** Changes in the activities of lipase during interaction with PLA MPs and PS MPs hydrolysis products collected after 2 hours of biodegradation. **f** Schematic diagram of the synthesis of fluorescein isothiocyanate (FITC)-Labeled PLA polymer. **g** Changes in the fluorescence signal in the supernatant during the biodegradation FITC-Labeled PLA MPs by lipase. Data are presented as the mean  $\pm$  SEM of triplicates \* $p < 0.05$ , \*\* $p < 0.01$  (ANOVA). Abbreviations: MPs, microplastics; PLA, poly-lactic acid.



**Figure 2**

**Characterization of PLA-nanoplastic formation.** **a** Concentration of PLA-nanoplastics measured by nanoparticle tracking analysis (NTA). **b** AFM-IR (atomic force microscope-infrared spectroscopy) spectra of PLA-nanoplastics. **c** Dynamic Light Scattering (DLS) diameter of PLA-nanoplastics with different biodegradation time by lipase. **d** Transmission electron microscope (TEM) of PLA-nanoplastics. **e** Effect of dilution and tween 20 (1%) on the size of PLA-nanoplastics. **g** Microscopic images of aggregation of PLA oligomers with MW of 900 g/mol at the concentration of 5 mg/mL. **h** Gel permeation

chromatography (GPC) analysis of PLA hydrolysis products. **i** HPLC-Q-TOF-MS analysis of PLA hydrolysis products. **j** Trajectories depicting the aggregation of PLA oligomers with 8 units at 0 and 100 ns. PLA oligomers were shown as spherical model (carbon, cyan; oxygen, red; hydrogen, white). **k** Conformation of the complex formed between PLA oligomers with 8 units and lipase at 0 and 100 ns. Lipase was shown as ribbon model, PLA oligomers was shown as stick model. Carbon, pink; oxygen, red; hydrogen, white. Ser153, Asp177 and His264 were shown as element stick model (carbon, cyan; nitrogen, blue; oxygen, red). Data are presented as the mean  $\pm$  SEM of triplicates.

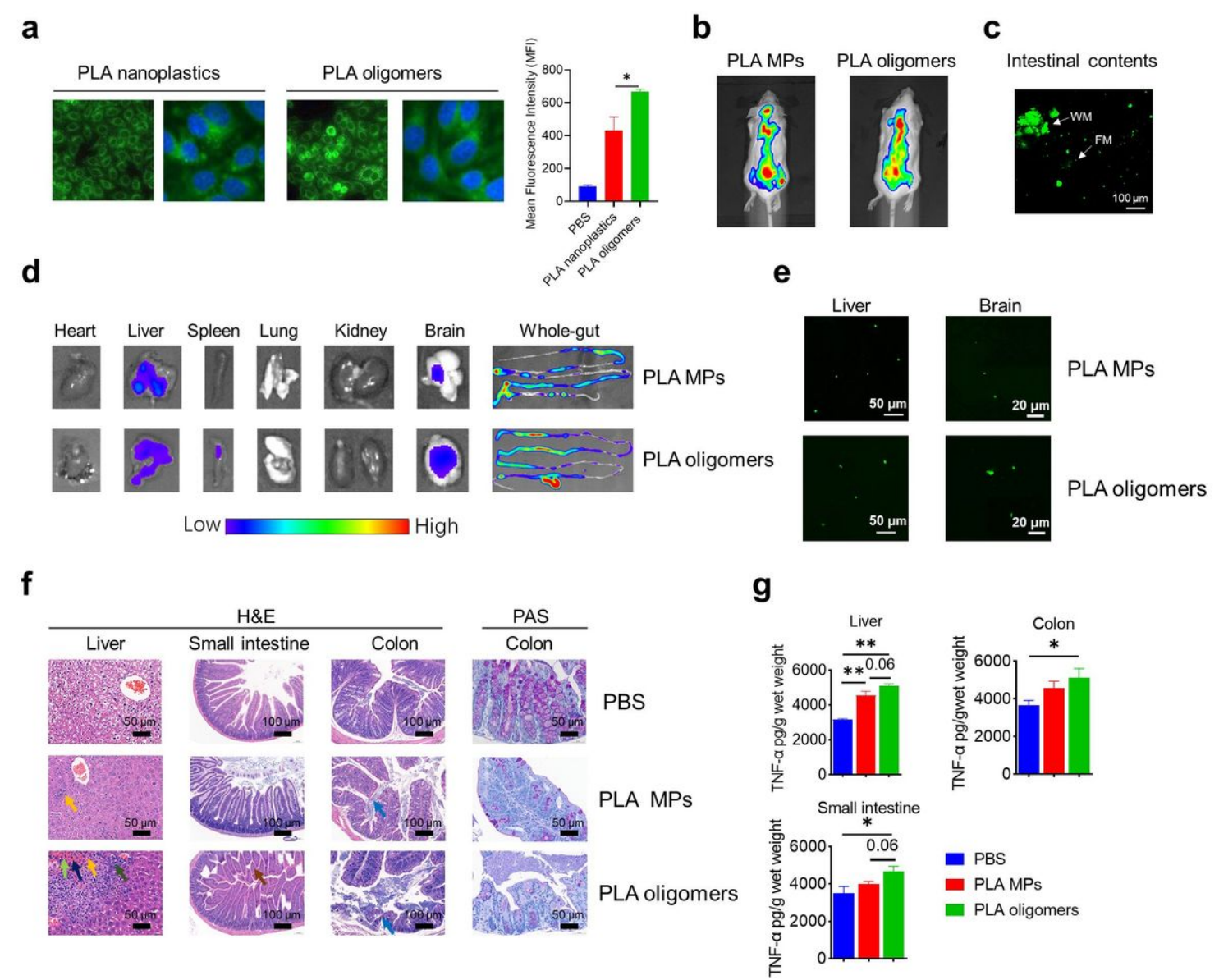


**Figure 3**

**Biodistribution and histopathology of PLA nanoplastics/oligomers *in vitro* and *in vivo*.** **a** Uptake of fluorescently labelled PLA-nanoplastics and PLA-oligomers by HepG2 cells. Mean fluorescence intensity (MFI) was also analyzed. **b** Biodistribution of PLA hydrolysis products and PLA oligomers in mice. **c** Fluorescent images of fragmented PLA MPs in intestinal content. WM: whole microplastics, FM:

fragmented microplastic. **d** Fluorescent images of tissues excised from mice. **e** Accumulation of PLA hydrolysis products and PLA oligomers in mouse tissues (liver and brain). **f** Representative images of H&E-stained (neutrophils, yellow arrows; lymphocytes, light green arrows; red blood cells, black arrows; cells infiltration, teal arrows; intestinal villi, brown arrows; lamina propria separation, blue arrows) liver, small intestine, and colon sections. Colon sections were stained with periodic acid-Schiff (PAS) to measure goblet cell hyperplasia and mucosal secretion. **g** ELISA results for TNF- $\alpha$  in liver, small intestine, and colon tissues. *In vitro*: Data presented as the mean  $\pm$  SEM of triplicates. *In vivo*: Data presented as mean  $\pm$  SEM of 5 mice per group. \* $p < 0.05$ , \*\* $p < 0.01$  (ANOVA).

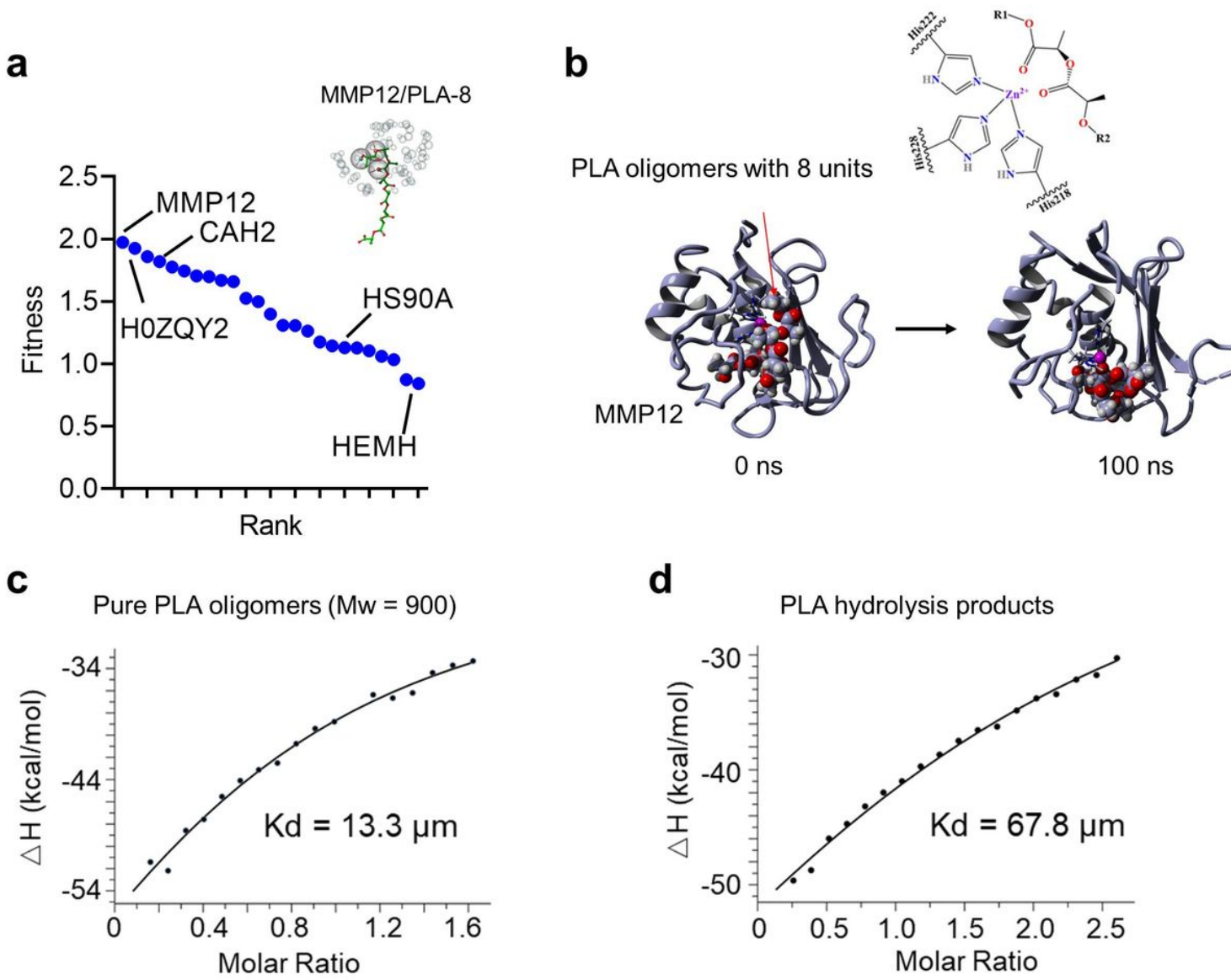


**Figure 4**

**PLA oligomers inactivate MMP12.** **a** A pharmacophore model used to screen for 16,646 potential target proteins against the PLA oligomers with 8 units, among which top 25 matched proteins were plotted. The highest scores aligned with MMP12. PLA oligomer is represented by sticks. **b** Conformation of the complex formed between PLA oligomers with 8 units and MMP12 at 0 and 100 ns. MMP12 shown as

lightblue ribbon model, PLA oligomers shown as spherical model. Carbon, lightblue; oxygen, red; hydrogen, white. His218, His222 and His228 shown as lightblue stick model (carbon, lightblue; nitrogen, blue), Zinc ions shown as purple spherical model. **c, d**  $K_d$  values of the interaction between MMP12 and PLA oligomer (MW: 900 g/mol) **c** and PLA hydrolysis products **d** were determined using ITC binding assay.

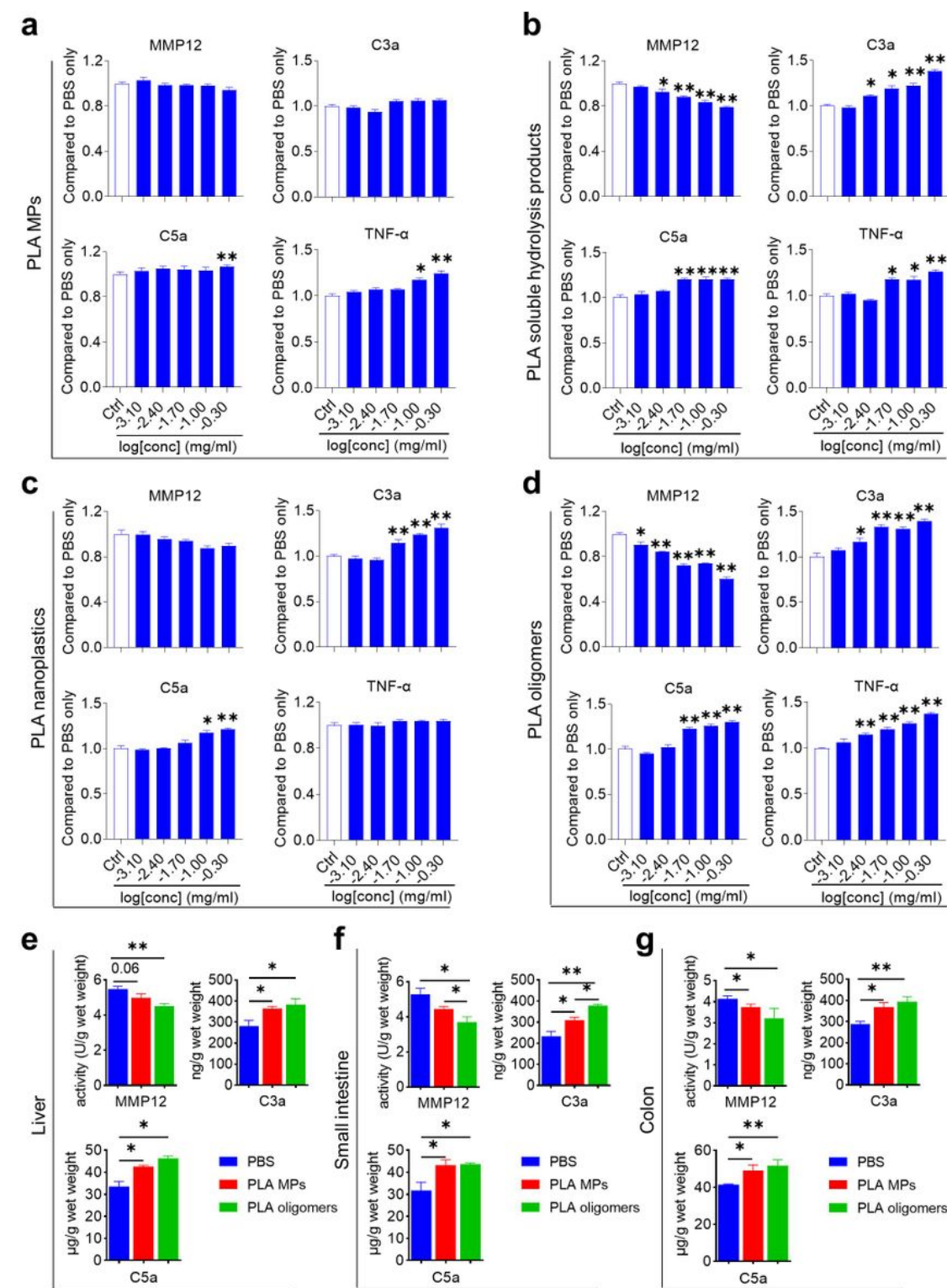
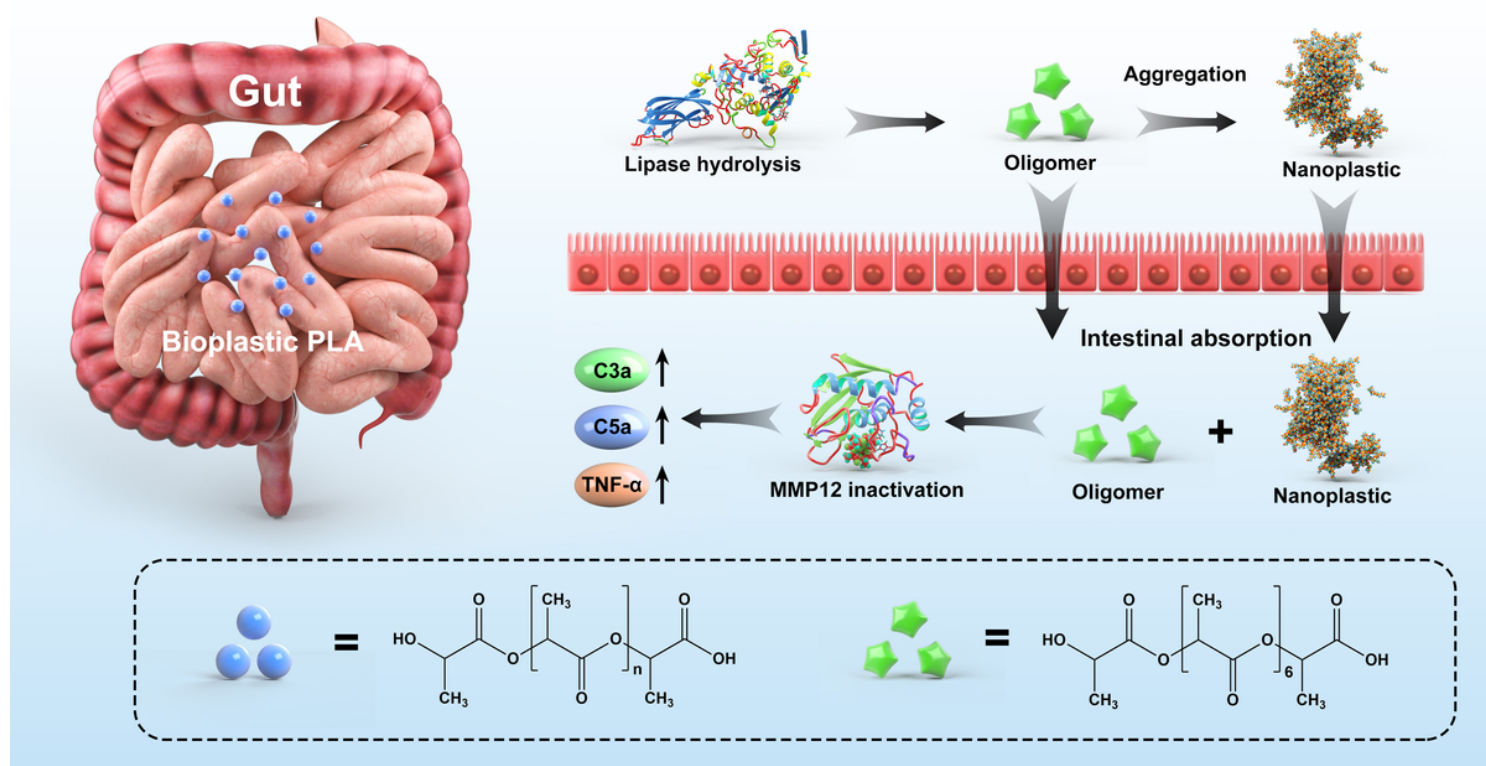


Figure 5

**MMP12 inactivation-mediated intestinal inflammation induced by PLA oligomer.** **a-d** Effects of PLA MPs on: **a**, PLA soluble hydrolysis products **b**, PLA-nanoplastics **c**, PLA-oligomers **d** on MMP12 activity, and C3a, C5a, TNF- $\alpha$  production in RAW 264.7 cells. **e-g** ELISA results for MMP12 activity, and C3a, C5a production in liver **e**, small intestine **f**, and colon tissues **g**. *In vitro*: Data presented as the mean  $\pm$  SEM of triplicates compared with DMSO vehicle control. *In vivo*: Data presented as mean  $\pm$  SEM of 5 mice per group. \* $p < 0.05$ , \*\* $p < 0.01$  (ANOVA).



**Figure 6**

**Graphic summary.** When PLA bioplastics are ingested, gastrointestinal lipase rapidly depolymerizes them into oligomers which could either exist as themselves or self-assemble as nanoplastics, permeating the gastrointestinal tract and entering the circulation. Oligomers could further inactivate MMP12 leading to inflammation in the intestinal system, providing new insight into ingested PLA bioplastics induced inflammation.

## Supplementary Files

This is a list of supplementary files associated with this preprint. Click to download.

- [Supportinginformation.docx](#)